

Light Wave Coupled Flat Panel Displays and Solid-State Lighting Using Hybrid Inorganic/Organic Materials

Andrew J. Steckl, *Fellow, IEEE*, Jason Heikenfeld, *Member, IEEE*, and Steven C. Allen, *Student Member, IEEE*

Invited Paper

Abstract—We present a review of light-emitting materials and devices that combine inorganic and organic lumophores and hosts. The essence of this hybrid inorganic/organic (I/O) approach is to combine materials, structures and devices from each category in such a way as to obtain best-of-both-worlds performance. The combination of high power/high efficiency inorganic light pump sources with high conversion efficiency organic lumophores is discussed in detail. In this type of Hybrid I/O device, near-ultraviolet (UV) or blue pump light is selectively converted to various visible colors based on the molecular structure of each lumophore. Since the lumophores are optically pumped their reliability is greatly increased compared to electrically pumped organic emitters. Methods for coupling the light from pumps to lumophores include direct path excitation (DPE) and light wave coupling (LWC). DPE uses one pump per lumophore pixel, which allows for active matrix style addressing, but requires large arrays of pumps. LWC uses either a single source or a small number of pump sources. To obtain pixelation for Hybrid I/O LWC devices we have developed a novel electrowetting switching method. Examples of Hybrid I/O displays and solid-state lighting are discussed.

Index Terms—Electrowetting, flat panel displays, hybrid inorganic/organic, light wave coupling (LWC), lumophore, optical pumping, solid-state lighting.

I. INTRODUCTION

A GREAT variety of light-emitting materials and excitation mechanisms have been developed for displays and lighting applications. Two major factors are changing the landscape of light emission and causing a reevaluation of existing options as well as a search for new alternatives. In the past decade, the advent of flat panel displays for computer and television applications has greatly increased the investigation of many methods of light emission and control, including the light valve approach [as in liquid crystal displays (LCDs)], the gas plasma emission approach, and solid-state emissive approaches (such as inorganic and organic light-emitting devices—LEDs).

Manuscript received February 14, 2005; revised May 27, 2005. This work was supported in part by the U.S. Army Research Office and U.S. Army Research Laboratory.

A. J. Steckl and S. C. Allen are with the Nanoelectronics Laboratory, University of Cincinnati, Cincinnati, OH 45221 USA (e-mail: a.steckl@uc.edu; allensc@email.uc.edu).

J. Heikenfeld is with the Extreme Photonix LLC, Cincinnati, OH 45219-2374 USA (e-mail: jheikenf.extremephotonix@biostart.org).

Digital Object Identifier 10.1109/JDT.2005.853269

Display applications have put a premium on emitting materials with high brightness, efficiency, contrast, and accurate RGB chromaticity. In addition, device technology requirements for displays include a thin form factor, the ability to scale up to large overall dimensions for TV-type applications and to scale down to small pixel dimensions for microdisplay applications. More recently, the solid-state lighting initiative has also brought attention to the need for low cost, high power sources with very high efficiency and good color rendering. Given this complex web of requirements, it is not likely that a single type of light-emitting material or a single device technology can emerge as the single dominant solution.

We present a review of specific combinations of inorganic and organic light-emitting materials for applications in displays and solid-state lighting. As shown in Fig. 1, we can classify the materials as “pumps” (short wavelength light sources: near-UV, violet, or blue) or “lumophores” (longer wavelength conversion materials: red, green, and blue—RGB). In general, both organic and inorganic materials can serve as pumps, using electron-hole recombination across the gap between conduction (CB) and valence bands (VB) for inorganic semiconductors or between the lowest unoccupied (LUMO) to the highest occupied molecular orbitals (HOMO) in organic materials. The lumophores are typically rare earth and transition metals, as well as organic and organometallic compounds. They operate by absorbing the pump photons, leading to an excited energy state (ES, or promotion to the LUMO) followed by radiative relaxation to the ground state (GS, or demotion to the HOMO) and the emission of lower energy photons.

Several combinations, which have received much attention, are shown in Fig. 1. They include: 1) the combination of inorganic wide bandgap semiconductors (WBGS) (such as III-N’s and II-VI’s) or oxide hosts (such as sulfates, gallates, silicates, etc.) with rare earth (RE) lumophores, for example, red emission from Eu-doped GaN LED in Fig. 1(a); 2) organic hosts containing RE or inorganic lumophores; 3) organic LEDs either directly emitting visible light and/or converting to longer wavelengths by pumping organic lumophores, as shown in Fig. 1(b); and 4) organic lumophores emitting at visible wavelengths [Fig. 1(c)] through conversion of high energy photons emitted by inorganic WBGS LEDs [Fig. 1(d)] or fluorescent lamps [Fig. 1(e)]. The combination of RE lumophores in inorganic

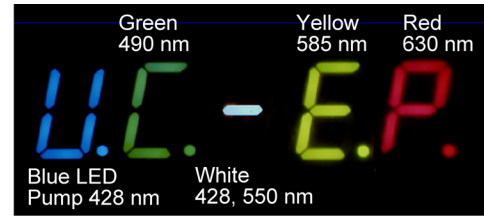
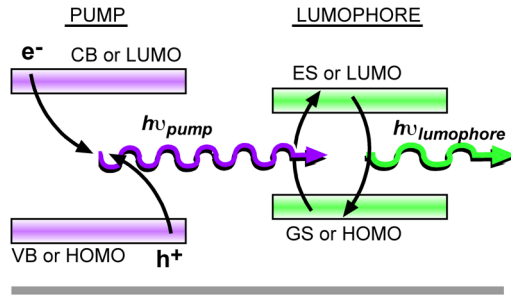


Fig. 3. Organic lumophores excited by InGaN LED's 7-segment arrays. (Color version available online at <http://ieeexplore.ieee.org>.)

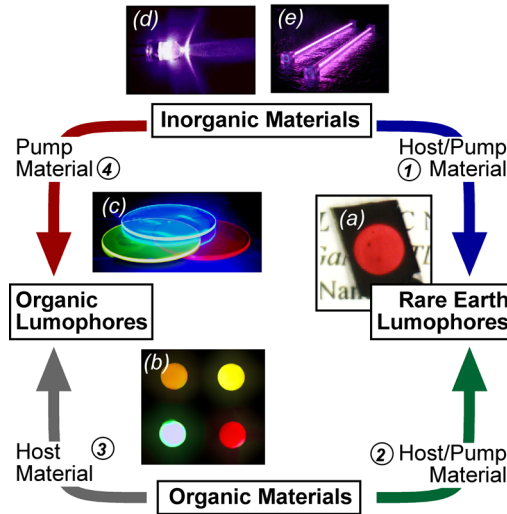


Fig. 1. Combinations of inorganic and organic pumps or host materials and lumophore materials. (Color version available online at <http://ieeexplore.ieee.org>.)

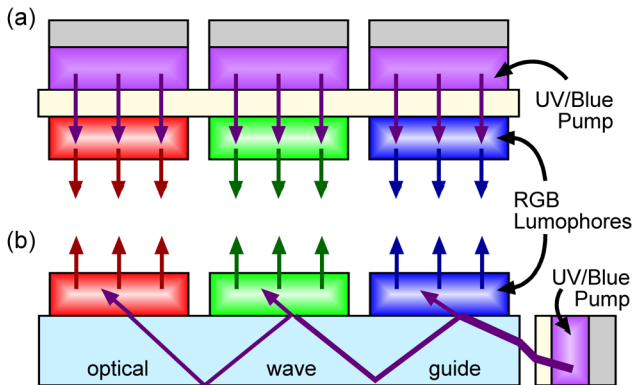


Fig. 2. Hybrid I/O approaches. (a) Direct path excitation. (b) Light wave coupling (LWC). (Color version available online at <http://ieeexplore.ieee.org>.)

hosts has been pursued for several decades [1], most recently in III-N semiconductors [2]. The science and technology of organic (including metalorganic) lumophores in organic hosts has been under vigorous development for the past decade and progress is continuing at a rapid pace [3].

In this paper, we discuss the hybrid inorganic/organic (I/O) approach [4], [5] which combines high power, long lifetime inorganic LEDs with organic lumophores that have very high photon conversion efficiency, adjustable emission color, can be easily deposited over large areas, and are very low cost. Two implementations of the Hybrid I/O approach are shown in Fig. 2: (a) the direct path excitation (DPE) approach, wherein there is an inorganic pump for each organic lumophore; (b) the light

wave coupling (LWC) approach, which uses an optical waveguide to transmit the pump photons from a single (or a few) inorganic pump to an array of lumophore pixels. For the LWC approach, light propagation in the waveguide is governed by Snell's law of refraction at the interface between two media of refractive index n_1, n_2

$$n_1 \sin \theta_1 = n_2 \sin \theta_2 \text{ or } n_x = \sqrt{n_w^2 - \sin^2 \theta_{\text{PUMP}}} \quad (1)$$

where θ_{PUMP} is the angle at which the pump illuminates the edge of the waveguide and n_x is the refractive index of a lumophore material in contact with the surface of the waveguide (n_w). Ideally, n_x is matched to n_w such that coupling is achieved for all values of θ_{PUMP} .

This review covers optical properties of the organic lumophores, light wave coupling of the inorganic pump source and the organic lumophore, and provides preliminary results on Hybrid I/O displays and lighting devices.

II. LIGHT-EMITTING MATERIALS AND DEVICES

In the basic Hybrid I/O approach, photons from ultraviolet (UV)- or blue-emitting inorganic LEDs are absorbed by organic lumophores, which in turn emit RGB photons based on their specific chemical structure and composition. Organic lumophore RGB color conversion under optical pumping with inorganic (InGaN) LEDs is illustrated in Fig. 1(c). The overall photon efficiency of the color conversion process combines the inherent ("internal") quantum efficiency of the lumophore (η_{int}) with the photon outcoupling efficiency (η_{oc}) from the material (leading to the external quantum efficiency— η_{ext}). The power conversion efficiency has to also take into account the difference in energy between the pump photons and the emitted photons (the Stokes shift, η_{St}).

The equations for these efficiency parameters are given by

$$\eta_{\text{ext}} = \eta_{\text{oc}} \times \eta_{\text{int}} = \eta_{\text{oc}} \times \frac{\text{emitted photon flux}}{\text{injected carrier flux}} \quad (2a)$$

$$\eta_{\text{St}} = \frac{h\nu_{\text{out}}}{h\nu_{\text{in}}} = \frac{\gamma_{\text{pump}}}{\gamma_{\text{emit}}}, \quad \eta_{\text{pc}} = \eta_{\text{oc}} \times \eta_{\text{int}} \times \eta_{\text{St}} \quad (2b)$$

$$\eta_{\text{oc}} = \frac{(1 - \cos \theta_c)}{2} \eta_c \approx \frac{1}{4n_{\text{lumo}}^2}, \quad \theta_c = \sin^{-1} \left(\frac{n_{\text{air}}}{n_{\text{lumo}}} \right) \quad (2c)$$

where n_{lumo} and n_{air} are the refractive indices of the lumophore material and air, respectively.

A simple, but effective, implementation of an "active matrix" Hybrid I/O display uses blue InGaN 7-segment alphanumeric indicators as the pump sources in conjunction with various organic lumophores. In the example shown in Fig. 3, the InGaN

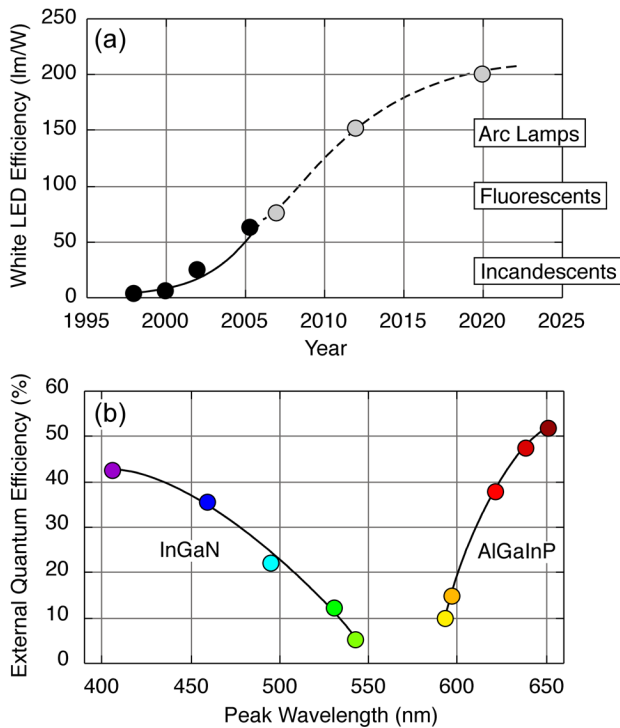


Fig. 4. (a) Historical development (solid line-actual, dash line-projected) of white LED luminous efficiency [6]; (b) External quantum efficiency vs. wavelength [7] for various inorganic light sources. (Color version available online at <http://ieeexplore.ieee.org>.)

LEDs emit at 428 nm (as shown in the leftmost unit), while the other units are converted to green (with peak emission at 490 nm), yellow (585 nm), red (630 nm), and white (dual peaks at 428, 550 nm) by various combinations of organic lumophores.

A variety of options are available for both the inorganic short wavelength pump sources and for the organic lumophores. For UV/blue sources one can utilize either nitride-based LEDs or fluorescent lamps. As shown in Fig. 4(a), the luminous efficiency [6] of white lumophore-converted blue LEDs is increasing rapidly and in coming years is expected to overtake fluorescent lighting, which is the current efficiency leader in generation of white light at ~ 80 lm/W. Since the light generation mechanism for Hybrid I/O is the same as that used for white LEDs, it is fully expected that the luminous efficiency for LED-pumped Hybrid I/O should also follow the projections shown in Fig. 4(a). The external quantum efficiency for InGaN and AlGaInP LEDs [7] is shown in Fig. 4(b). Limitations in the range of III–V alloy compositions and in the availability of true epitaxial substrates are the cause for the reduced performance in the 500–600-nm regime, often referred to as the ‘green gap.’ Fortunately for Hybrid I/O, near-UV, violet, or blue pumping is accomplished with InGaN LEDs which require only low (or no) In content. Through efficient lumophore conversion, Hybrid I/O bridges the green gap. For example, a 90% conversion efficient green lumophore pumped by a violet (405 nm) LED (with low In content) should provide an external quantum efficiency near 40%. This is a fourfold improvement over a green InGaN LED which requires higher In content. LED packages are projected to eventually match the maximum lumen output and cost per lumen of cold-cathode fluorescent lamps (CCFL).

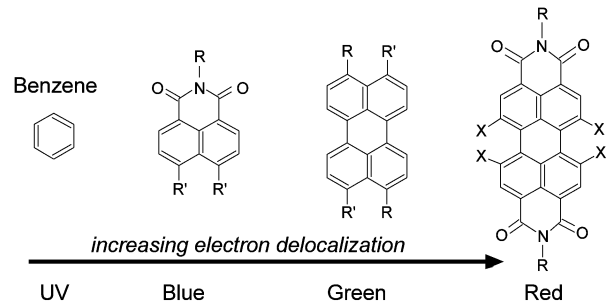


Fig. 5. Benzene as a building block for organic lumophores.

However, to meet near-term needs in high lumen Hybrid I/O applications, we have developed a proprietary cold-cathode lamp well suited for use as a lumophore pump source. This cold-cathode lamp has a pure violet emission with an emission full-width at half-maximum of < 30 nm.

The basis of many organic lumophores is the benzene molecule (C_6H_6) shown in Fig. 5, whose conjugated bonding results in delocalized molecular orbitals that absorb and emit UV light at ~ 180 and ~ 250 nm, respectively. In general, an increase in the size of the conjugated molecule or in the number of benzene rings results in a decrease (increase) of the emitted photon energy (wavelength). Many organic lumophores can be viewed as combinations of benzene rings with functional groups that further tailor their optical properties by modifying the electron distribution through groups that either accept or donate electrons. Examples of organic lumophores are shown in Fig. 5: naphthalimide-based molecule for blue emission, and two perylene-based molecules for green and red emission. The central 5-ring structure is the basic perylene molecule. The photoluminescence (PL) spectral characteristics of RGB lumophores are shown in Fig. 6(a). Using an InGaN LED emitting at 400 nm to pump the lumophores, emission peaks are observed at 430, 540, and 620 nm for each lumophore. The Stokes shift between the optical absorption and emission spectra is illustrated in Fig. 6(b) for the blue lumophore.

Table I contains typical performance values obtained for lumophores incorporated into PMMA solutions (normally $\sim 1\%$) and pumped with an InGaN LED at 400 nm: (a) the ‘red’ lumophore is the most inherently efficient, with internal QE as high as 98%; (b) the ‘green’ lumophore usually has a lower efficiency because it has a lower threshold for significant re-absorption of the green photons and emission at longer wavelengths (red shift); (c) the ‘blue’ lumophore has QE levels (~ 90 –95%) between those displayed by red and green lumophores, but has the highest power efficiency because of the smaller Stokes shift. Clearly, the high performance of the lumophores is one of the assets of the Hybrid I/O approach. Interestingly, the Hybrid I/O concept of optimum combinations of inorganic and organic materials is also being pursued in electronic devices [8].

III. LIGHT WAVE COUPLING DISPLAYS

The advantages of Hybrid I/OTM are directly applicable to displays. As previously discussed (see Fig. 2) a monochrome UV, violet, or blue inorganic display panel can be converted with organic lumophores to create a full-color display panel.

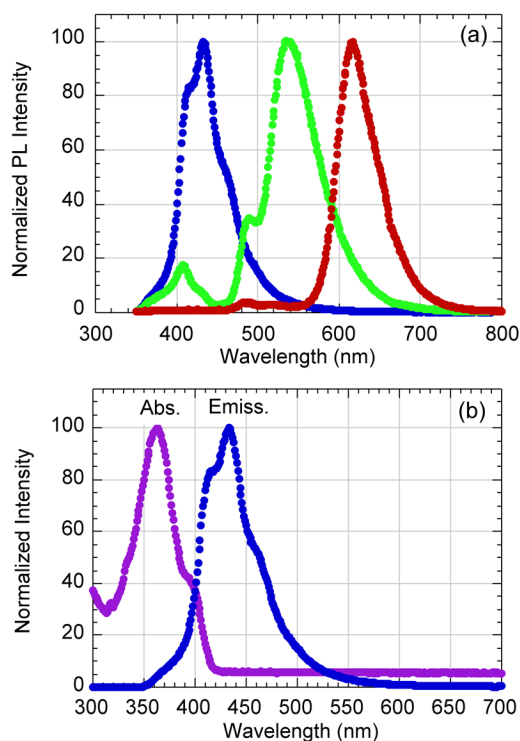


Fig. 6. Spectral characteristics of perylene lumophores. (a) PL spectra of RGB lumophores and (b) absorption and emission spectra of blue lumophore. (Color version available online at <http://ieeexplore.ieee.org>.)

TABLE I
VIOLET TO RGB CONVERSION EFFICIENCY OF SELECTED ORGANIC LUMOPHORES

Color	Peak Eff. (nm)	External Power Eff. (%)	External Quantum Eff. (%)	Internal Quantum Eff. (%)
Red	640	9	14	95
Green	540	9	12	80
Blue	430	12	13	90

This can provide cost and performance advantages, an example being lumophore converted inorganic electroluminescence of HDTV panels [9]. However, to fully reap the benefits of Hybrid I/O for displays requires use of the most efficient and robust inorganic pump sources available. These highly efficient sources are only found in the form of point sources (LEDs) or line sources (cold-cathode-fluorescent lamps, CCFLs). This renders the DPE approach using LEDs or CCFLs impractical for creating a high-pixel count 2-D display panel [see Fig. 2(a)]. Therefore, to allow use of LEDs and CCFLs we have chosen to utilize the novel LWC method [see Fig. 2(b)] for displays. As shown in Fig. 7(a), in LWC for displays an inorganic violet source (~ 400 nm) pumps light into a large waveguide plate constructed of glass or transparent polymer. By edge mirroring the waveguide, light is then able to traverse the waveguide numerous times covering distances as long as tens of meters before 50% light attenuation. This effectively creates a plate which can provide high-power violet pump light at any position on the waveguide surface. A full-color display panel can then be created by optically coupling or decoupling an array of red, green, and blue emitting lumophores. As seen in Fig. 7(b), the

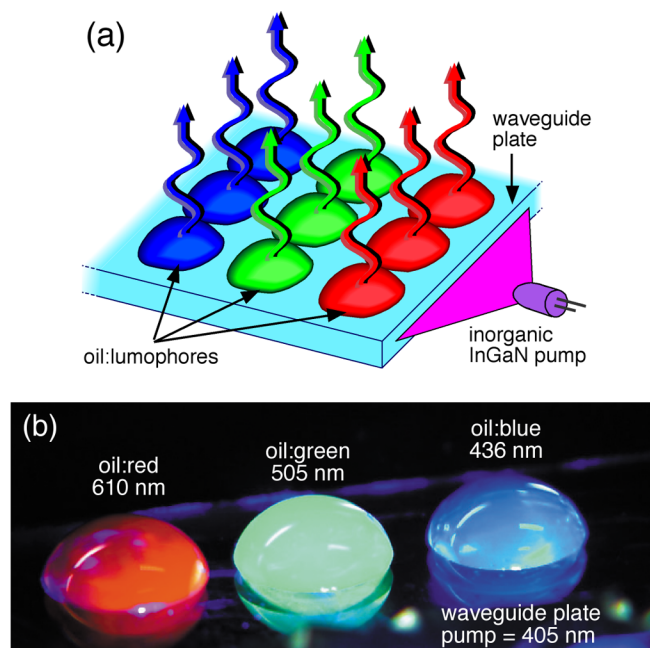


Fig. 7. LWC displays. (a) Overall concept for a flat panel display. (b) Photographs of liquid oil:lumophores on an LWC waveguide plate edge-pumped with 405 nm InGaN LEDs. (Color version available online at <http://ieeexplore.ieee.org>.)

lumophores can be introduced into a special oil which is index matched to the waveguide [see (1)].

Through careful choice of materials, the lumophores doped into the oil also exhibit the high optical performance of lumophores doped into solid polymers. A liquid oil:lumophore solution allows for use of novel electro-wetting (EW) ON/OFF pixel switching, which will be discussed in further detail in Section IV. Loss-less EW switching was chosen for LWC since standard switching methods such as liquid crystal are only ~ 5 – 10% optically efficient, even in the fully ON state (maximum light transmission). This basic premise of combining Hybrid I/O, LWC, and EW for a display panel is projected to provide record-breaking potential for display brightness and efficiency.

EW is an electrostatic microfluidic technology that has recently found application in numerous compelling new photonic technologies [10], [11]. EW finds broad applicability in photonics since it is the first microfluidic technology to provide: 1) very low operating power; 2) extremely fast speed for a fluidic technology (~ 1 ms); and 3) good stability of operation. The basic EW mechanism is shown in Fig. 8. The liquid repelling nature of an electrically insulating hydrophobic dielectric can be counteracted by application of an electric field (polarization) across the dielectric. As shown in the photo of Fig. 8(a), a highly polar liquid such as water (high surface tension, $\gamma \sim 73$ dynes/cm) beads up on a ~ 1 μm thick clear hydrophobic dielectric of amorphous Teflon (low surface energy, $\gamma \sim 16$ dynes/cm). By applying a voltage between the droplet and a transparent electrode beneath the hydrophobic dielectric, the droplet rapidly [12]–[14] (\sim ms) wets the surface [Fig. 8(b)]. The process is fully reversible and capacitive so that no power is consumed while the droplet is held in either the wetted or de-wetted state of actuation. In simplest terms, application of voltage causes electrostatic attraction of the

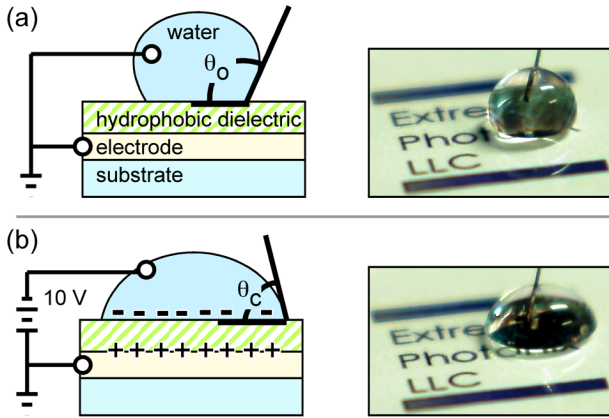


Fig. 8. Diagrams and photos of the basic electrowetting mechanism. A polar liquid such as water, which (a) normally has a large contact angle on a hydrophobic dielectric, can be electrostatically modulated (b) to wet the dielectric and decrease in contact angle. (Color version available online at <http://ieeexplore.ieee.org>.)

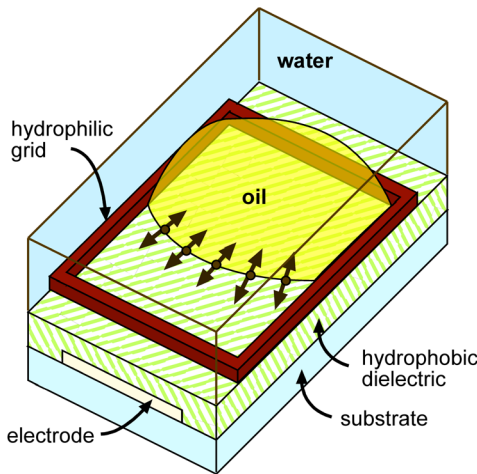


Fig. 9. Basic structure for creating isolated EW cells to be used as pixels in an LWC display. (Color version available online at <http://ieeexplore.ieee.org>.)

water surface to the hydrophobic dielectric. Droplet actuation is measured via the water contact angle (θ_C) that is found at the vertex of the water/air/hydrophobic dielectric interfaces. Water contact angle can be predicted using the EW equation

$$\cos \theta_C = \cos \theta_0 + \frac{\epsilon_o \epsilon_r}{2z\gamma} (V)^2 \quad (3)$$

where θ_0 is the contact angle without applied bias, V is the applied bias, ϵ_r and z are the relative dielectric constant and thickness of the hydrophobic dielectric, and γ is the water surface tension. This droplet form of EW is not applicable to LWC displays but is presented in order to promote initial understanding of the basic EW mechanism.

EW for LWC displays utilizes a second fluid that is nonpolar (an oil, $\gamma \sim 27$ dynes/cm) and therefore is not soluble with the polar water fluid. Suitable oils include simple organic liquids such as alkane hydrocarbons or nonorganic liquids such as silicone oils. This form of EW, shown in Fig. 9, is referred to as competitive EW [15]. Due to interfacial surface tension relationships, the oil always situates itself between the water and

hydrophobic dielectric. The oil can be thought of as behaving similar to the air around the droplet in Fig. 8 (or conversely, an air bubble trapped between the water and hydrophobic dielectric). Hence, at the vertex between the water/oil/hydrophobic dielectric the water has a large contact angle. In addition to being nonpolar, the oil must also be highly electrically insulating. Therefore, as voltage is applied to the system, only the interface between the hydrophobic dielectric and water experiences significant capacitive charge up. The result is that as the voltage increases, the increasing wetting of the hydrophobic dielectric by the water layer forces the oil layer to contract. The same relationship in (3) applies, with the substitution of the interfacial surface tension of the water/oil for the water-only surface tension. For displays, the oil must be confined laterally so as to define a pixel structure [16]. As shown in Fig. 9, this can be achieved through use of a hydrophilic grid. This hydrophilic grid can be formed via simple photolithographic means since common photoresist materials are acrylic-based and have a high surface energy of ~ 40 dynes/cm. This high surface energy attracts the water layer and prevents lateral spreading of the oil droplet. The hydrophilic grid can further limit EW-induced contraction/expansion of the oil layer to one direction. This can be achieved by modifying the surface energy of the side-walls of the hydrophilic grid, by electrode patterning, or by spatially modifying the thickness (capacitance) of the hydrophobic dielectric.

IV. LIGHT WAVE COUPLING PIXELATION

As shown in Fig. 10, EW pixel structures for LWC displays were constructed on a glass substrate that also serves as a waveguide. On the waveguide are deposited a thin transparent indium-tin-oxide (ITO) ground electrode, a $\sim 1.0 \mu\text{m}$ thick hydrophobic dielectric, and a reflective optical cladding. The hydrophobic dielectric and transparent electrode have refractive indices greater than or equal to that of the waveguide and therefore also participate in waveguide propagation of violet pump light. The optical cladding does not participate in violet light propagation and causes internal reflection of pump light. The hydrophobic dielectric and cladding both have surface energies less than 20 dynes/cm so that strong water contact angle modulation (oil movement) may be achieved. Individual LWC pixels are defined by patterning hydrophilic grid lines which are $\sim 1 \times 3$ mm in perimeter. For a simple test setup, a common deionized water ($> 16 \text{ M}\Omega\text{-cm}$) is dosed over the entire LWC pixel array and a bias electrode wire is placed into the water layer. It is important to note that in a video display panel the water layer would be commonly grounded and the ITO patterned to allow addressing of individual pixels. Following water dosing, ~ 100 to ~ 300 nL of ~ 1 wt.% lumophore-doped oil is inserted into each LWC pixel. The oil layer thickness is tens of micrometers. The waveguide is edge-illuminated with violet (~ 405 nm) InGaN LEDs. Waveguide edges are mirrored with Al reflectors for violet light recycling.

Refractive index values for various materials are labeled in parentheses in Fig. 10, and are critical to understanding operation of the LWC pixel [see (1)]. Under conditions of zero applied bias [see Fig. 10(a)] to the water layer, interfacial surface tensions cause the oil:lumophores to form a continuous film between the water and hydrophobic layers. In this configuration, violet

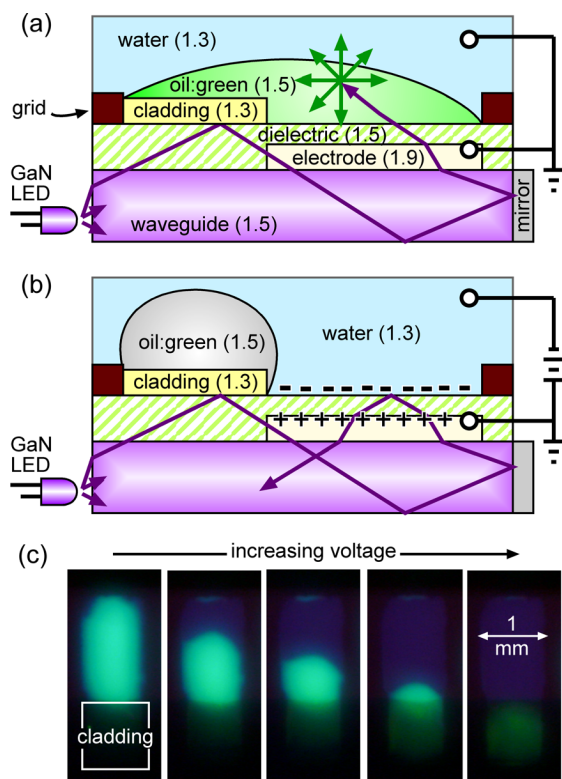


Fig. 10. Cross-sectional diagram and operation of EW pixels cells for LWC displays [7] in the ON (a) and OFF (b) states of emission. Refractive indices for materials are given in parenthesis. Top-view photographs of 3 mm² LWC pixels in operation (c). (Color version available online at <http://ieeexplore.ieee.org>.)

light from the waveguide refracts through the ITO and the hydrophobic insulator, and penetrates the oil:lumophore layer. The lumophores in the oil are then excited by the violet pump light and radiate intense visible light. This results in an LWC pixel in the ON state. As shown in Fig. 10(b), the fluorescence emission from the LWC pixel is switched OFF via EW. As voltage is applied to the water it is electrostatically attracted toward the hydrophobic insulator. This displaces the oil:lumophore layer onto the solid cladding layer. Now, at the upper surface of the hydrophobic dielectric, violet pump light encounters a complete optical cladding comprised of the solid optical cladding layer and the low index water layer. This complete cladding then prevents violet light from reaching the oil:lumophores. Progression of oil:lumophore movement and resulting luminance at several applied voltages is shown in the photographs of Fig. 10(c). This device configuration results in an LWC pixel in the OFF state. Additionally, pump light is recycled for use in adjacent LWC pixels in the ON state. Light recycling along with other high efficiency aspects of LWC are projected to result in a luminous efficiency which is more than an order of magnitude greater than that achievable for LCDs. Theoretical loss mechanisms and resultant net efficiency are compared for LCD and LWC displays in Table II. First, absence of RGB color filter loss of $\sim 70\%$ and polarizing media loss of $\sim 70\%$ provides LWC with an instant efficiency advantage over LCD. This advantage is further enhanced in most displays applications where the average percentage of pixels in the fully ON state is $< 50\%$. An LCD pixel simply absorbs and wastes light in the OFF-state, whereas as an LWC pixel recycles light in the OFF-state.

TABLE II
LWC VERSUS LCD PEAK THEORETICAL LUMINOUS EFFICIENCY COMPARISON

	LCD	LWC
Source	CCFL-80 lm/W	CCFL-80 lm/W
Waveguide	50% efficient	50% efficient
Polarizers	40% \times 80% (two)	100% (none)
Source Utilization		
10% pixels on	10%	60%
50% pixels on	50%	90%
100% pixels on	100%	100%
Color Filter	30%	100% (none)
Emission	100% (none)	80%
Net Efficiency		
10% pixels on	0.4 lm/W	19 lm/W
50% pixels on	2 lm/W	29 lm/W
100% pixels on	4 lm/W	32 lm/W

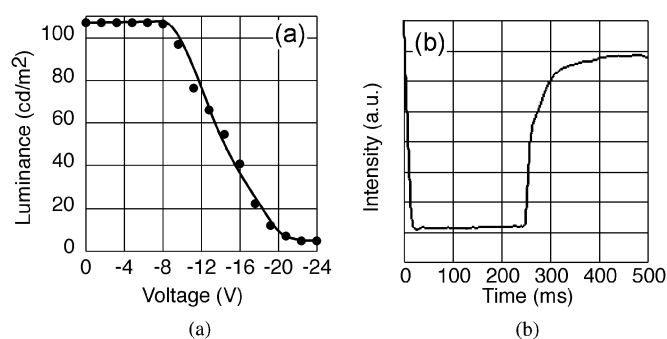


Fig. 11. (a) Luminance-voltage and (b) intensity-time characteristics for a 3 mm² LWC pixel [10].

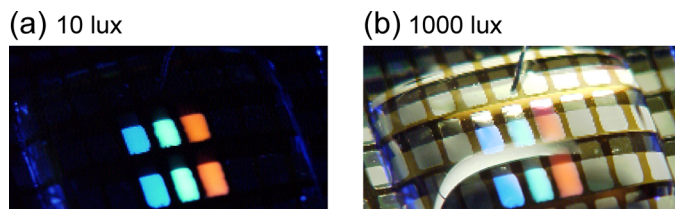


Fig. 12. Photographs of RGB LWC pixels in the ON state [10], shown in both dark (10 lux) and bright (1000 lux) ambient lighting conditions. (Color version available online at <http://ieeexplore.ieee.org>.)

The luminance-voltage characteristic of the LWC pixel is shown in Fig. 11(a). Modulation of the applied voltage allows for grayscale control of the pixel luminance. Pixel capacitance is very low ($\sim \text{nF/cm}^2$). Low capacitance along with the potential for low-voltage ($< 10 \text{ V}$) operation allows LWC pixels to be compatible with existing thin-film-transistor backplanes used in active matrix LCDs. Low voltage operation can be achieved through improved pixel design, surface energy/tension optimization, and/or through use of specialized surfactants. This should greatly expedite the commercial development of LWC displays. Current LWC pixels exhibit an ON/OFF contrast ratio of $\sim 20:1$. This contrast ratio is primarily limited by insufficient lensing for the InGaN LEDs. From the contrast ratio one can approximate that 5% of the violet LED light is introduced into the waveguide at an angle which exceeds the critical angle [(1)] at the hydrophobic dielectric ($n \sim 1.5$) interface with the water or cladding layers ($n \sim 1.3$ for both). This contrast should reach ratios of 100:1 with use of advanced side-emitting LED lenses or selective attenuation of large-angle guided violet light in the waveguide.

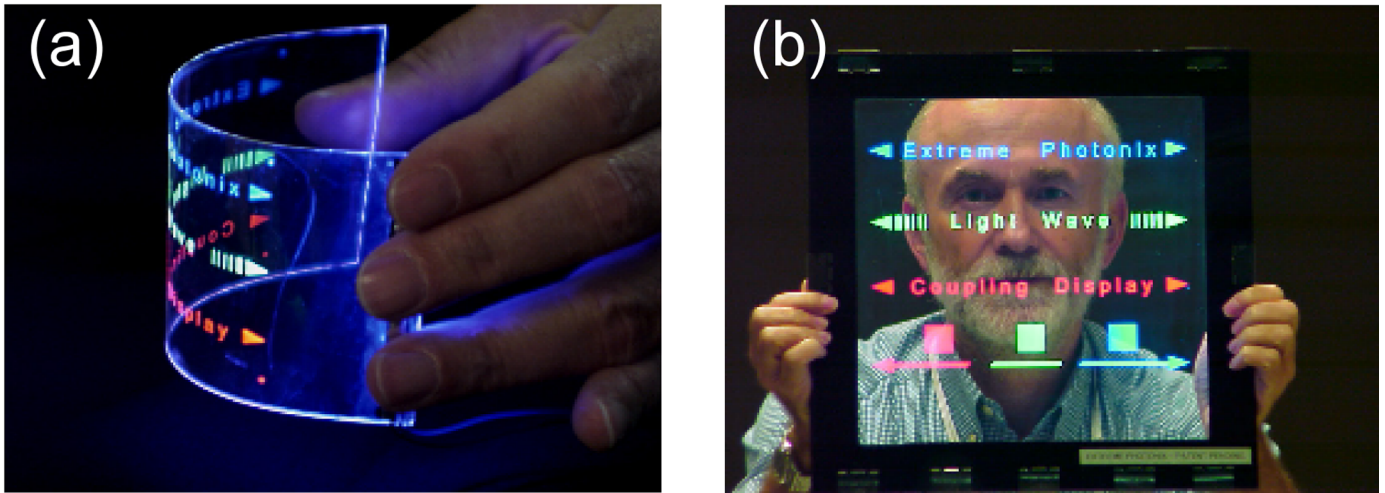


Fig. 13. (a) Flexible and (b) rigid LWC displays showing additional advantages of flexibility and transparency [11]. (Color version available online at <http://ieeexplore.ieee.org>.)

As shown in Fig. 11(b), LWC pixels are able to exhibit ON and OFF switching times ($1/e$) in the tens of milliseconds. The ON time is governed by electrowetting (electrostatic) forces whereas the OFF time is governed by purely capillary forces. Smaller geometry pixels allow for switching times of ~ 10 ms and will improve with development. Given that total-internal reflection requires cladding layers $>1 \mu\text{m}$ thick, aspect ratio consideration limits the minimum pixel size to about $\sim 10 \mu\text{m}$. By simply increasing the InGaN LED light intensity, luminance $>500 \text{ cd/m}^2$ has been measured from 15×30 arrays LWC devices. The photographs of Fig. 12 further reveal that full-color pixel operation is easily viewable under ambient lighting conditions ranging from very dark (10 lux) to very bright (1000 lux). Rapid scale-up of the basic LWC display concept has been achieved by printing of solid polymer host:lumophores on flexible [see Fig. 13(a)] and large rigid [see Fig. 13(b)] waveguide sheets of various sizes up to $300 \times 600 \text{ mm}$. These demonstrator panels reveal both scalability and color performance on large size waveguides. In addition, these panels also reveal two exciting features of LWC displays: flexibility and transparency. It is important to note that achieving flexibility for LWC displays is more straightforward than in LCDs since LWC pixels possess no cell-gap dependence and are stable in any physical orientation. Flexible waveguide materials include a variety of modified acrylic or silicone polymer systems. Current LWC research is now partially focused on scaling up the electrowetting pixel results of Fig. 12 to larger scale nonelectrowetting demonstrators like those shown in Fig. 13.

V. HYBRID I/O LWC SOLID STATE LAMPS

The Hybrid I/O concept has also been developed for solid-state lighting (SSL) applications [17]. Hybrid I/O for SSL provides the following advantages: 1) high maximum conversion efficiency; 2) low materials cost; 3) large selection of available conversion colors; and 4) good color rendering. Additionally, the LWC approach can be incorporated in the Hybrid I/O solid-state lighting approach. An example of Hybrid I/O LWC for SSL is shown in Fig. 14. This combination further provides: 1) spatial separation of pump and lumophores for improved

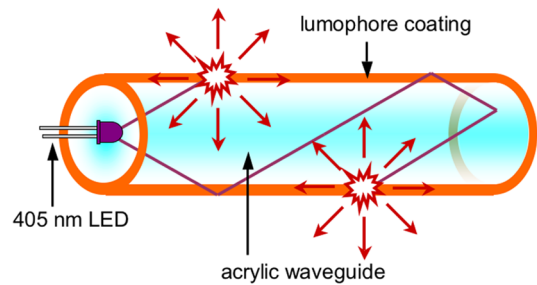


Fig. 14. Diagram of Hybrid I/O lamp design and operation using the LWC method for pump light distribution. (Color version available online at <http://ieeexplore.ieee.org>.)



Fig. 15. Photographs of (left to right) violet, blue, green red, and white Hybrid I/O lamps. The violet lamp has no lumophore and appears in false color (photographed with 3-color CCD). (Color version available online at <http://ieeexplore.ieee.org>.)

stability through reduced thermal degradation; 2) elimination of phosphor scattering; 3) improved white point control; and 4) 2-D and 3-D lamp form factors (beyond point source configuration). In these LWC lamps, pump (UV, violet, or blue) light is distributed through a transparent waveguide to organic lumophores that convert the pump wavelength to the desired color. LWC Hybrid I/O lamps with cylindrical geometry are shown in Fig. 15. Examples of violet, blue, green, red, and white Hybrid I/O lamps are included. The photographs of the lamps give

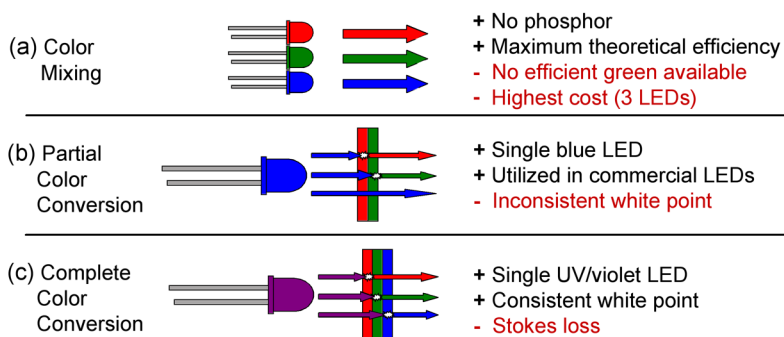


Fig. 16. Three main approaches to solid-state lighting. (Color version available online at <http://ieeexplore.ieee.org>.)

some false coloration due the 3-primary color limitation of the charge-coupled device (CCD) camera used for image capture. The geometry of the lamps shown in Fig. 15 was inspired by fluorescent tubes, with the possible advantage of using existing lamp fixture designs.

For development of white lamps, there are several potential combinations of pump source and lumophores. Leading approaches are shown in Fig. 16 and include the following: (I) *Color mixing*—combining the output from three RGB LEDs. The color mixing approach has the advantage of highest maximum luminous efficiency (no conversion loss). However, the absence of efficient LEDs in the green region of the spectrum currently limits this approach. Furthermore, this is the most expensive option since it requires use of three LEDs per lamp. (II) *Partial color conversion*—a blue pump source is partially lumophore-converted to yellow. The remaining unconverted blue pump light transmits through the lumophore, and combines with the yellow-converted light to form white light. This is the most commercially prevalent approach, utilizing an InGaN LED chip coated with a yellow inorganic phosphor (YAG:Ce). (III) *Complete color conversion*—the output from a single UV or violet LED is completely absorbed and converted by two or more lumophores to white light. For hybrid I/O lamps the complete color conversion approach is utilized since it provides the best white point reproducibility. Furthermore, this approach can take advantage of high external quantum efficiency InGaN LEDs. For example, quantum efficiency of 43% for 405-nm violet LEDs has been reported [18].

To explore their potential for white lighting, several advanced white Hybrid I/O lamps were fabricated and analyzed for color temperature, efficiency, and loss mechanisms. The lamps utilized a 405-nm LED pump and conversion via multiple lumophores to increase spectral coverage for good color rendering. The highest efficiency lamp exhibited Commission Internationale de l'Éclairage (CIE) coordinates (0.34, 0.32), indicative of a correlated color temperature (CCT) of ~ 5100 K. The emission spectrum of this lamp is plotted in Fig. 17 along with that from an ideal 5100 K blackbody. The CIE diagram of Fig. 18 indicates the coordinates of several Hybrid I/O white lamps. The various CCTs were obtained for lamps that were identical except for composition of the lumophores. For reference, color temperature standards are also indicated on the diagram. The 5100-K lamp exhibited a luminous efficiency of 16 lm/W and a wall-plug power efficiency of 6.3%. Significant efficiency improvements are

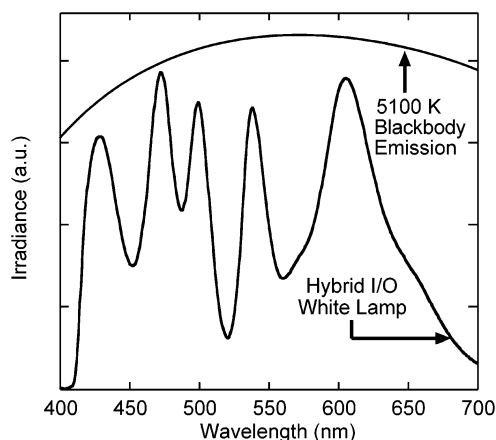


Fig. 17. Hybrid I/O lamp spectrum compared to that of a blackbody lamp with a CCT of 5100 K.

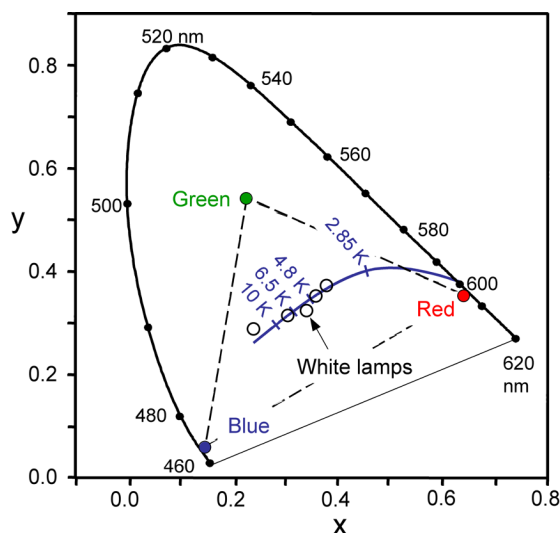


Fig. 18. CIE diagram listing the color coordinates of the blue, green, red, and white Hybrid I/O lamps. Coordinates of blackbodies at selected temperatures are also shown. (Color version available online at <http://ieeexplore.ieee.org>.)

expected in several areas: (a) increased power efficiency of the pump LED; (b) decreasing the Stokes shift by moving to longer pump wavelength (410–450 nm); (c) light outcoupling; (d) dye spectrum.

The Optoelectronics Industry Development Association (OIDA) has set a solid-state lighting luminous efficiency target [6] of 75 lm/W for the year 2007. In addition, OIDA has outlined specific recommendations for the wavelength conversion

approach used here. These include a wall-plug chip efficiency of 46%, lumophore and “package” (i.e., outcoupling) quantum efficiencies of 75% each, and Stokes efficiency of 73%. The total luminous efficiency of Hybrid I/O lamps is expressed as

$$\eta_L = \eta_{\max}\eta_{\text{LED}}\eta_{\text{int}}\eta_{\text{St}}\eta_{\text{oc}} \quad (4)$$

where the maximum luminous efficiency (η_{\max}) is determined from the lamp spectrum assuming 100% power conversion efficiency. The LED electrical-to-optical power conversion efficiency (η_{LED}) was measured separately with an integrating sphere and is 15.8% at 10 mA or approximately 1/3rd of the OIDA recommendation. The product of the lumophore and package efficiencies ($\eta_{\text{int}}\eta_{\text{oc}}$) of the Hybrid I/O lamp is 54%, very close to the 56% OIDA recommendation. The Stokes conversion efficiency (η_{St}) matches the roadmap value of 73%. Primarily because the 405 nm pump LED is significantly less efficient than the OIDA roadmap recommendation, the luminous efficiency falls short of current OIDA goals. However, it is important to note that utilizing a 405 nm LED with 46% power efficiency into the current lamp would yield 47 lm/W. External quantum efficiencies as high as 43% for 405 nm LEDs were reported [18] in 2003, so it is reasonable to expect that the 46% power efficiency goal will be met or exceeded by 2007. In addition to the use of higher efficiency violet LEDs, the lamp performance can be improved by modifying the lumophore composition to better match the theoretical RGB white point primaries at 459, 539, and 604 nm.

The maximum luminous efficiencies for color mixing by three 20 nm bandwidth LEDs have been calculated [19]. Given a CCT of 5000–5500 K and a CRI of 80, a maximum luminous efficiency of 368–378 lm/W can be obtained with LEDs at wavelengths of 459, 539, and 604 nm. This efficiency should be considered as an upper bound because the peak wavelengths likely cannot be precisely met, and bandwidths are generally larger with lumophores than LEDs. However, mixtures of lumophores should have improved color rendering due to more complete spectral coverage than that possible by using only LEDs. An important characteristic of all solid-state lighting devices is their degradation with time under various operating conditions. White light sources using InGaN LEDs and inorganic phosphors have been shown (for a discussion of lifetime characteristics, see [20]) to have lifetimes approach 100 000 h, with a strong dependence on thermal management. We expect that similar lifetimes are obtainable with Hybrid I/O solid-state lighting.

VI. SUMMARY AND CONCLUSIONS

In this paper we have reviewed the fundamentals and applications of hybrid inorganic/organic light-emitting devices that combine near UV/blue inorganic light pumps with organic lumophores, which convert the pump light to visible emission. The Hybrid I/O approach allows the device designer to take advantage of the independent optimization of pump sources and lumophores, thus producing a best-of-both-worlds technology. This inherent versatility combined with the high efficiency of both elements of the device leads to a very attractive approach for several applications. While significant research and development is required for Hybrid I/O devices to realize their full potential in solid-state lighting and display applications, early

device results are very promising. In Hybrid I/O lamps, new optical designs of the LWC lamps are being investigated, along with the design of the optimal lumophore white emitting blend. In Hybrid I/O displays, new cell designs and improved materials (fluorescent lumophores and hydrophobic insulator coatings) are currently being explored. In conclusion, we believe that the Hybrid I/O concept will produce a compelling new technology platform in the near future.

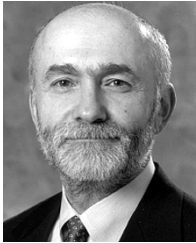
ACKNOWLEDGMENT

The authors are pleased to acknowledge the encouragement of J. Zavada, D. Morton, and E. Forsythe, and the support of the members of the UC NanoLab, Cincinnati, OH.

REFERENCES

- [1] A. Kitai, Ed., *Solid State Luminescence*. London, U.K.: Chapman & Hall, 1993.
- [2] A. J. Steckl, J. C. Heikenfeld, D. S. Lee, M. Garter, C. C. Baker, Y. Q. Wang, and R. Jones, “Rare-earth-doped GaN: Growth, properties and fabrication of electroluminescent devices,” *IEEE J. Select. Top. Quantum Electron.*, vol. 8, no. 4, pp. 749–766, Jul. 2002.
- [3] J. Shinar, Ed., *Organic Light Emitting Diodes*. New York: Springer, 2004.
- [4] F. Hide, P. Kozodoy, S. P. DenBaars, and A. Heeger, “White light from InGaN/conjugated polymer hybrid light-emitting diodes,” *Appl. Phys. Lett.*, vol. 70, no. 20, pp. 2664–2666, 1997.
- [5] S. Guha, R. A. Haight, N. A. Bojarczuk, and D. W. Kisker, “Hybrid organic-inorganic semiconductor-based light emitting diodes,” *J. Appl. Phys.*, vol. 82, no. 8, pp. 4126–4128, 1997.
- [6] J. Y. Tsao, Ed., (2002) *Light Emitting Diodes for General Illumination*. Optoelectronics Industry Association (OIDA), Washington, DC. [Online]. Available: www.oida.org
- [7] M. Krames, “Progress and future direction of LED technology,” presented at the Solid State Lighting Workshop, Arlington, VA, Nov. 2003.
- [8] M. Bonse, D. B. Thomasson, H. Klauk, D. J. Gundlach, and T. N. Jackson, “Integrated a-Si:H/pentacene inorganic/organic complementary circuits,” in *Int. Electron Devices Meeting Tech. Dig.*, Washington, DC, 1998.
- [9] X. Wu, D. Carkner, H. Hamada, I. Yoshida, M. Kutsukake, and K. Dantani, “Large-screen flat panel displays based on thick-dielectric electroluminescent (TDEL) technology,” in *Proc. Soc. Inf. Display*, vol. 35, Seattle, 2004, pp. 1146–1149.
- [10] J. Heikenfeld and A. J. Steckl, “Intense switchable fluorescence in light wave coupled electrowetting devices,” *Appl. Phys. Lett.*, vol. 86, no. 1, pp. 011 105–011 105-3, 2005.
- [11] —, “Liquid light—electrowetting emerging for displays,” *Inf. Displ.*, vol. 20, no. 11, pp. 26–31, Nov. 2004.
- [12] M. G. Pollack, R. B. Fair, and A. D. Shenderov, “Electrowetting-based actuation of liquid droplets for microfluidic applications,” *Appl. Phys. Lett.*, vol. 77, pp. 1725–1726, 2000.
- [13] J. Lee, H. Moon, J. Fowler, T. Schoellhammer, and C. J. Kim, “Electrowetting and electrowetting-on-dielectric for microscale liquid handling,” *Sensors Actuators A*, vol. 95, pp. 259–268, 2002.
- [14] E. Colgate and H. Matsumoto, “An investigation of electrowetting based microactuation,” *J. Vac. Sci. Tech. A*, vol. 8, pp. 3625–3633, 1990.
- [15] B. Janocha, H. Bauser, C. Oehr, H. Brunner, and W. Göpel, “Competitive electrowetting of polymer surfaces by water and decane,” *Langmuir*, vol. 16, pp. 3349–3354, 2000.
- [16] R. A. Hayes and B. J. Feenstra, “Video-Speed electronic paper based on electrowetting,” *Nature*, vol. 425, pp. 383–385, 2003.
- [17] D. A. Steigerwald, J. C. Bhat, D. Collins, R. M. Fletcher, M. O. Holcomb, and M. J. Ludowise, “Illumination with solid state lighting technology,” *IEEE J. Sel. Top. Quantum Electron.*, vol. 8, no. 2, pp. 310–320, Mar. 2002.
- [18] H. Kudo, Y. Ohuchi, T. Jyouichi, T. Tsunekawa, H. Okagawa, K. Tadatomo, Y. Sudo, M. Kato, and T. Taguchi, “Demonstration of high-efficient InGaN-based violet light-emitting diodes with an external-quantum efficiency of more than 40%,” *Phys. Stat. Sol. (a)*, vol. 200, no. 1, pp. 95–98, 2003.

- [19] Y. Ohno, "White LED simulator II," in *Light Emitting Diodes for General Illumination*, J. Y. Tsao, Ed., 2002, p. 12. [Online] Available: www.oida.org.
- [20] N. Narendran and Y. Gu, "Life of LED-based white light sources," *J. Display Technol.*, vol. 1, no. 1, pp. 167–171, Sep. 2005.



Andrew J. Steckl (S'70–M'73–SM'79–F'99) received the B.S.E. degree in electrical engineering from Princeton University, Princeton, NJ, in 1968, and the M.Sc. and Ph.D. Degrees from the University of Rochester, Rochester, NY, in 1970 and 1973, respectively.

In 1972, he joined the Honeywell Radiation Center, Lexington, MA, as a Senior Research Engineer, where he worked on new concepts and devices in the area of infrared detection. In 1973, he joined the Technical Staff of the Electronics Research Division of Rockwell International, Anaheim, CA. At Rockwell he was primarily involved in research on charge coupled devices. In 1976, he joined the Electrical, Computer and Systems Engineering Department at Rensselaer Polytechnic Institute in Troy, NY, where he developed a research program in microfabrication of Si devices. In 1981, he founded the Center for Integrated Electronics, a multi-disciplinary academic center focused on VLSI research and teaching, and served as its director until 1986. Since 1988, he has been with the Electrical and Computer Engineering Department of the University of Cincinnati as Ohio Eminent Scholar and Gieringer Professor of Solid State Microelectronics. At Cincinnati, he has built the Nanoelectronics Laboratory in the general area of semiconductor materials and devices for photonics. Current activities include GaN MBE growth, rare-earth-doped organic and inorganic luminescent devices, hybrid inorganic/organic materials and devices for flat panel displays and solid-state lighting. His research has resulted in over 330 publications and over 350 conference and seminar presentations.



Jason Heikenfeld (S'99–M'01) received the B.S. and Ph.D. degrees in electrical engineering with minors in both photonics and physics from the University of Cincinnati, Cincinnati, OH, in 1998 and 2001, respectively.

He is a scientist and co-founder at Extreme Photonix Corporation, Cincinnati, OH. His main duties at Extreme Photonix involve leading the research and development of novel hybrid display technologies. He has authored and coauthored over 100 publications in refereed journals, industry magazines, conference proceedings, and a book chapter. He is an inventor on several granted and pending U.S. patents.

Dr. Heikenfeld is a member of the IEEE Lasers and Electro-Optics Society, and the Society for Information Display.



Steven C. Allen (S'05) received B.S. degrees in physics and chemistry at Ohio University, Athens, in 2001, and the M.S.E. degree in electrical engineering from Princeton University, Princeton, NJ in 2003. He is currently working toward the Ph.D. degree in electrical engineering at the University of Cincinnati, Cincinnati, OH. In his doctoral study, he is focusing on novel lamp designs for solid-state lighting applications.